Defence Science Journal, Vol. 58, No. 1, January 2008, pp. 15-33

Trajectory Correction Flight Control System using Pulsejet on an Artillery Rocket

S.K. Gupta, S. Saxena, Ankur Singhal and A.K. Ghosh
Indian Institute of Technology, Kanpur–208 016

ABSTRACT

A trajectory correction flight control system is small and durable, and consists of a lateral pulsejet ring mounted on the rocket body. The pulsejet ring consists of a finite number of individual pulsejets. Each pulsejet on the ring imparts a single, short-duration, large force to the rocket in the plane normal to the rocket axis of symmetry. Lateral pulsejets are used by flight control system to assist the rocket to follow a pre-specified (command) trajectory. The trajectory-tracking flight control system computes the position error by comparing the measured position of the rocket with the pre-specified trajectory. In actual application, the position of the rocket could be measured using in-house inertial measurement unit (IMU) or by ground-based-tracking radar system located at the firing site. A study has been undertaken to explore the feasibility of reducing the impact point dispersion of a routinely-used artillery rocket using lateral pulsejets coupled to a trajectory correction flight control system. Simulation studies have been conducted to arrive at tuning parameters, namely the tracking error window size, the required elapsed time between the pulsejet firings and the angle of tolerance between the tracking error and the individual pulsejet force. Further, the robustness of the methodology wrt measurement noise has also been evaluated.

Keywords : Pulsejet, trajectory-tracking flight control system, impact point dispersion, trajectory-tracking window size, inertial measurement unit, trajectory correction flight control system

NOMENCLATURE

$c.g.$	Location of the centre of gravity of the rocket
C_A	Axial force coefficient
C_D	Drag force coefficient
C_{NA}	Normal force aerodynamic coefficient
C_X, C_Y, C_Z	Force coefficients in the X,Y,Z directions, respectively
C_l, C_m, C_n	Roll, pitch, and yaw moment coefficients, respectively
d	Rocket reference diameter
e_{thres}	Trajectory-tracking window size
I_{XX}, I_{YY}, I_{ZZ}	Moment of inertia of the rocket about the X, Y, Z-axes
L, M, N	Total applied moments about rocket mass centre expressed in the body reference frame
m	Mass of the rocket
n_j	Number of individual lateral pulsejet
n_{RX}, n_{RY}, n_{RZ}	i^{th} Main rocket motor direction cosines in the body frame
p, q, r	Components of the angular velocity vector of the projectile in the body reference frame

Received 01 November 2006, revised 26 February 2007

S	Rocket reference area
T	Main rocket thrust
V	Magnitude of the velocity vector of the mass centre of the projectile experienced with mean wind expressed in the body reference frame
T	Time constant
T_{ji}	i^{th} Lateral pulsejet thrust
T_R	i^{th} Main rocket motor thrust
t^*	Time of the most recent pulsejet firing
u, v, w	Components of the velocity vector of the mass centre of the composite body in the body reference frame
V_i	Magnitude of the velocity vector of the mass centre of the projectile experienced with mean wind expressed in the body reference frame
V_{MW}, σ_{MW}	Magnitude and wind factor of the mean atmospheric wind expressed in the initial reference frame
X, Y, Z	Total applied force components in the aft body reference frame
x, y, z	Components of the position vector of mass centre of the composite body in an inertial reference frame
$\overline{q}$	Dynamic pressure
α	Angle of attack
$ß$	Sideslip angle
θ_t	Angle between J_B and i^{th} pulsejet
ρ	Air density
ϕ, θ, ψ	Euler roll, pitch, and yaw angle of the projectile
Δ_{PJ}	Pulsejet firing duration
Δt_{thres}	Minimum required elapsed time between successive pulsejet firings
δ_{thres}	Pulsejet angle threshold

Subscripts

A	Aerodynamic contribution
J	Lateral pulsejet contribution
R	Main rocket thrust contribution
w	Rocket weight contribution

1. INTRODUCTION

Artillery rockets are used to support the personnel in contact with the enemy in the forward areas. The artillery has lived up to its reputation of softening the fiercely-defending enemy targets and thus making way for successful infantry assaults in the forward areas. The role of field artillery is to provide fire-support to other arms by backing up attacks, providing defensive fire, neutralising an enemy's gun emplacement and generally acting as a basis around which all other arms can operate. System accuracy is probably the most important consideration in an artillery system. Accuracy is measure of ability of the rocket to position the payload at a given point. Accuracy of the rocket in hitting the desired target depends on launching velocity irregularities due to variations in propellant mass, and metrological effects like ambient temperature density, head/tail wind, crosswind[1,2], etc. Dispersion caused by the variations in propellant mass can be greatly reduced by imposing proper manufacturing and assembly tolerance. Wind dispersion can be made less significant by the use of wind-compensation procedure which gives the launching azimuth or elevation angle, necessary, to achieve the desired trajectory[1-4]. Because artillery rockets exit the launcher with low velocity (30-40 m/s), any atmospheric disturbance (wind) presented to the rocket near the launcher creates relatively large angle of attack, leading to aerodynamic jump and increased impact point disperssion[1-5]. Furthermore, main rocket motor thrust during the initial portion of the flight tends to amplify the effect of initial transverse and angular perturbations on dispersion[1-4].

Conventional approach, hitherto, for understanding the inflight behaviour of the rocket was to develop the mathematical models that could predict all elements of the trajectory from launch to target. To this purpose, it becomes essential that all forces, moments affecting the flight of the projectile are accounted

for in a well-defined mathematical form[1-7]. Beginning with the most simple but relatively inaccurate mathematical model, more and more sophisticated models of increasing accuracy such as point mass model, modified point mass model and 6 degrees-of-freedom model have been developed[1]. However, even the best of these proposed models have their limitations due to their inability to model all of the problem variables adequately. Further, the trajectory model requires a large number of aerodynamic coefficients (linear/nonlinear) as input and the estimates available for these coefficients are not always accurate or reliable[8]. The limitations of the mathematical trajectory models so far used for predicting the performance of artillery rocket has necessitated designers to look at an alternative approach to reduce the inaccuracies.

The increasing demand for high-performance artillery rockets, including surgical removal of select targets, necessitates the use of a low-cost control mechanism to enhance its single-shot kill probability (SSKP)[2]. Technology involving microelectromechanical sensors, coupled with a suitable control mechanism could advantageously be used to enhance the SSKP of an unguided rocket[2]. Electronic industries routinely use pulse width and pulse-frequency modulation to arrive at different control methodologies for linear or low-order nonlinear systems[9-15].

The use of minimum-time optimal control schemes using pulse response was demonstrated[16]. The use of lateral pulsejets to improve the target dispersion performance of a projectile has been investigated by Harkins and Brown[9]. They used a set of lateral pulsejets to marginalise the off-axis angular rates of the projectiles just after exiting the launcher. Thanat and Coetello[2] demonstrated that the impact point dispersion of a direct-fire rocket could be drastically reduced with a ring of appropriately-sized lateral pulsejets, coupled to a trajectory-tracking flight control system. A trajectory-tracking flight control system[2] is small and durable, and consists of a lateral pulsejet ring mounted on the rocket body. The pulsejet ring consists of a finite number of individual pulsejets. Each pulsejet on the ring imparted a single, short-duration, large force to the rocket in the plane normal to the rocket axis of symmetry.

Lateral pulsejets were used by flight control system to assist the rocket to follow a pre-specified (command) trajectory. The trajectory-tracking flight control system computes the position error by comparing the measured position of the rocket with the pre-specified trajectory. The position-error vector in the inertial frame is computed using feedback from position and orientation sensors. It is assumed that the position and orientation sensors feedback is perfect, that is not corrupted by noise, bias or cross-axis sensitivity[2].

The flight control system performs a sequence of checks that govern firing of individual lateral pulsejet to effectively reduce the position error of the rocket in the flight[2]. Further, parametric studies that considered the effect of the tuning parameters, namely the number of pulsejets, pulsejet impulse and trajectory-tracking window size on impact point dispersion are presented[2]. Further, it is suggested that the tuning parameters that are specific to a given rocket have to be evaluated using pulsejet logic[2]. Pulsejet-firing logic is engaged when the trajectory-tracking error exceeded specific threshold. Effective implementation of this concept[2] largely depends on correctness of trajectory prediction model used, strength of pulsejet force (T_j), number of individual pulsejets (N_j), optimal time gap between the two consecutive pulsejet fires (Δt) and pulsejet angle threshold (δ). Further, it is also important to identify the part of the flight path during which operation of pulsejet results in efficient reduction in position error to achieve the desired impact point.

In actual application, the position of the rocket could be measured using in-house inertial measurement unit (IMU) or by ground-based-tracking radar system located at the firing site. Although, many-a-times, the use of ground-based radar system gets limited by the nonavailability of line of sight due to geographical constraints. However, in both the cases, presence of measurement noise, bias, etc are unavoidable and many-a-times could cause serious implementation problem.

Following the methodology[2], a study has been undertaken to explore the feasibility of reducing the impact point dispersion of a routinely-used artillery rocket using lateral pulsejets coupled to a

trajectory-tracking flight control system. The example artillery rocket, chosen for this study, achieves a maximum range of around 20 km when fired at an elevation angle of 50^{o}. However, this class of artillery rockets shows large dispersion when fired at low-launching angles. Simulation studies have been conducted to arrive at tuning parameters, namely the tracking error window size, the required elapsed time between the pulsejet firings and the angle of tolerance between the tracking error and the individual pulsejet force. This study tries to estimate the numerical values[2] of the tuning parameters required to reduce the impact point dispersion of the chosen example artillery rocket by applying pulsejet logic. Further, the robustness of the methodology wrt the measurement noise has also been evaluated for the example artillery rocket.

2. DIRECT-FIRE TRAJECTORY PREDICTION MODEL

To investigate the ability of a lateral pulsejet for reducing the impact point dispersion, a numerical simulation employed in this study consists of a rigid body and 6 degrees-of-freedom model typically utilised inflight dynamic modelling of projectiles[1,2]. A schematic of the direct-fire rocket configuration with major elements of the system identified is given in Fig.1. The degrees of freedom include three position components of the mass centre of the rocket, as well as three orientation angles of the body. The equations of motion[12] are provided in Eqns (1-4).

$$\begin{bmatrix} \dot{u} \\ \dot{v} \\ \dot{w} \end{bmatrix} = \begin{bmatrix} X/m \\ Y/m \\ Z/m \end{bmatrix} - \begin{bmatrix} 0 & -r & q \\ r & 0 & -p \\ -q & p & 0 \end{bmatrix} \begin{bmatrix} u \\ v \\ w \end{bmatrix} \quad (1)$$

$$\begin{bmatrix} \dot{\phi} \\ \dot{\theta} \\ \dot{\psi} \end{bmatrix} = \begin{bmatrix} 1 & \sin\varphi\tan\theta & \cos\phi\tan\theta \\ 0 & \cos\phi & -\sin\phi \\ 0 & \sin\phi\sec\theta & \cos\phi\sec\theta \end{bmatrix} \begin{bmatrix} p \\ q \\ r \end{bmatrix} \quad (2)$$

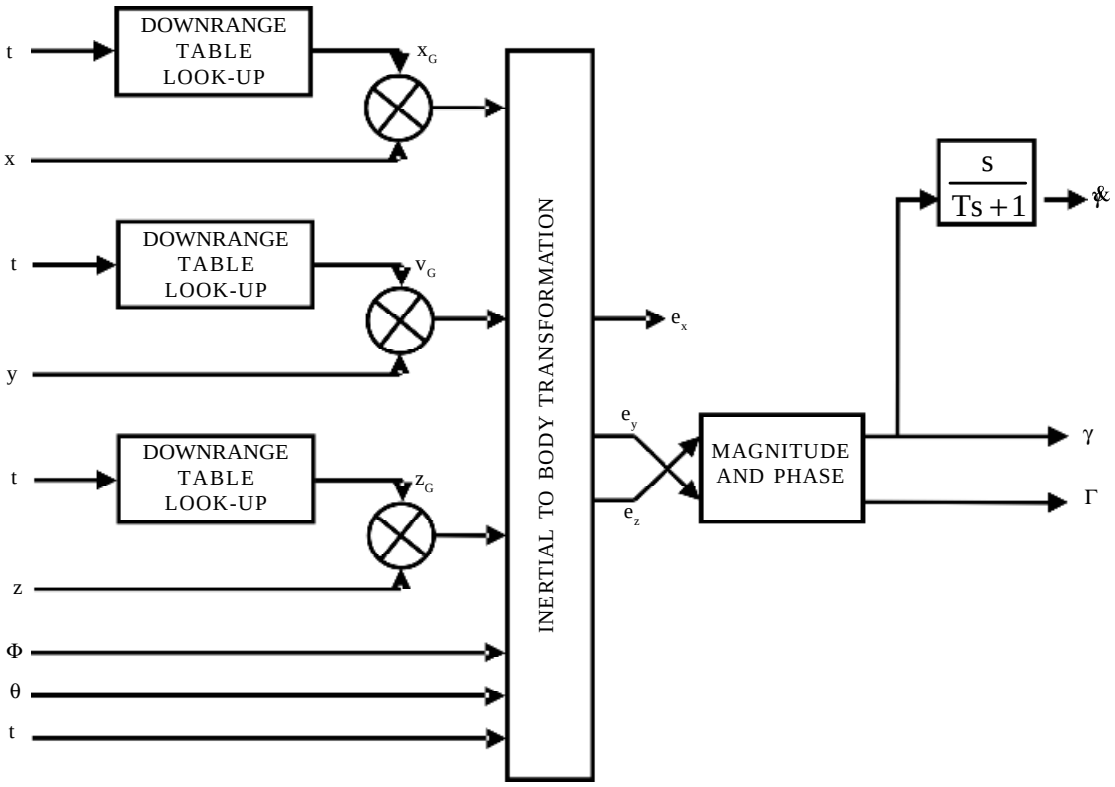

Figure 1. Schematic of trajectory-tracking flight control system.

$$\begin{bmatrix} \dot{p} \\ \dot{q} \\ \dot{r} \end{bmatrix} = \begin{pmatrix} I_{xx} & I_{yx} & I_{zx} \\ I_{xy} & I_{yy} & I_{zy} \\ I_{xz} & I_{yz} & I_{zz} \end{pmatrix}^{-1} \left[\begin{Bmatrix} L \\ M \\ N \end{Bmatrix} - \begin{pmatrix} 0 & -r & q \\ r & 0 & -p \\ -q & p & 0 \end{pmatrix} \begin{pmatrix} I_{xx} & I_{yx} & I_{zx} \\ I_{xy} & I_{yy} & I_{zy} \\ I_{xz} & I_{yz} & I_{zz} \end{pmatrix} \begin{Bmatrix} p \\ q \\ r \end{Bmatrix} \right] \tag{3}$$

In the modelling of equation of motion, the cross-product of inertia is considered. However, in the case due to nonavailability of the cross-product inertia values, these terms have been neglected and only the diagonal elements of the inertia matrix in Eqn 3 have been considered.

$$\begin{bmatrix} \dot{x} \\ \dot{y} \\ \dot{z} \end{bmatrix} = \begin{pmatrix} \cos\theta\cos\psi & \sin\phi\sin\theta\cos\psi - \cos\phi\sin\psi & \cos\phi\sin\theta\cos\psi + \sin\phi\sin\psi \\ \cos\theta\sin\psi & \sin\phi\sin\theta\sin\psi + \cos\phi\cos\psi & \cos\phi\sin\theta\sin\psi - \sin\phi\cos\psi \\ -\sin\theta & \sin\phi\cos\theta & \cos\phi\cos\theta \end{pmatrix} \begin{Bmatrix} u \\ v \\ w \end{Bmatrix} \tag{4}$$

The applied loads in Eqn (3) can be expressed[2] as follows:

$$\begin{bmatrix} X \\ Y \\ Z \end{bmatrix} = mg \begin{Bmatrix} -\sin\theta \\ \sin\phi\cos\theta \\ \cos\phi\cos\theta \end{Bmatrix} + \left(\frac{-\pi}{8} \rho V^2 d^2 \right) \begin{Bmatrix} C_{x0} + C_{x2} \left(v_A^2 + W_A^2 \right) / V_A^2 \\ C_{NA} \dfrac{v_A}{V_A} \\ C_{NA} \dfrac{W_A}{V_A} \end{Bmatrix}$$

$$+ \begin{Bmatrix} T_x \\ T_y \\ T_z \end{Bmatrix} + \sum_{\tau=1}^{n_j} T_{ji} \begin{Bmatrix} 0 \\ -\cos\left[2\pi(i-1)/n_j\right] \\ -\sin\left[2\pi(i-1)/n_j\right] \end{Bmatrix} \tag{5}$$

The net resultant force in the body-axis is the sum of gravity, aerodynamic, main motor rocket thrust and pulsejet forces[2]. Pulsejet force is molded as a constant because the lateral pulsejets are active over a very short duration of time when compared to the timescale of a complete rocket trajectory.

The total rolling, pitching and yawing moments are expressed as sum of moments due to aerodynamic and pulsejet force:

$$\begin{bmatrix} L \\ M \\ N \end{bmatrix} = \begin{Bmatrix} L_A \\ M_A \\ N_A \end{Bmatrix} + \begin{Bmatrix} L_J \\ M_J \\ N_J \end{Bmatrix} \tag{6}$$

The moments due to lateral pulsejet force (L_j, M_j, N_j) are computed with a cross-product between the distance vector from centre of gravity of the rocket and the location of the specific-force and the force itself. The moments due to aerodynamic forces are modelled using the conventional definition of stability derivatives:

$$L_A = \frac{1}{2} \rho V^2 S d \left[C_{l_p} \frac{pd}{2V} + C_{l_\delta} \delta \right] \tag{7}$$

$$M_A = \frac{1}{2}\rho V^2 Sd\left[C_{m_\alpha}\alpha + C_{m_q}\frac{qd}{2V}\right] \quad (8)$$

$$N_A = \frac{1}{2}\rho V^2 Sd\left[C_{n_\beta}\beta + C_{n_r}\frac{rd}{2V}\right] \quad (9)$$

The trajectory model [Eqns (1)-(9)] requires a large number of aerodynamic coefficients as input. For example rocket, these coefficients have been generated using exhaustive wind tunnel tests. Wind tunnel tests were conducted on a 5/12th scale model of the rocket to obtain the aerodynamic coefficients. Tests were conducted using trisonic wind tunnel (1.2 m x 1.2 m) at the National Aeronautical Laboratories, Bangalore. The slender rocket model consists of a frustum of an ogive nose and has a body length of about 2.8 m. The model has four wrap-around fins fixed at the tail portion with a cant angle of around 1^o to the axis of the model. The fins have a trapezoidal shape.

The aerodynamic forces and moments were measured using six-component (3.81 cm diameter) internal strain gauge balance. The base pressures were measured using the two tubes located at the model base and connected to the suitable transducers with a range ± 10 psid. The wind tunnel tests on the rocket model were conducted ranging from 0.6 M to 3.0 M. The nominal Mach numbers of the tests were 0.6, 0.8, 0.9, 1.0, 1.1, 1.2, 1.4, 1.7, 2.0, 2.5 and 3.0. The test program covered an angle of attack ranging from - 4 to 20^o. Typical variations of force and moment coefficients with Mach number and angle of attack are presented in Fig. 2. The estimated values of aerodynamic coefficients obtained through wind tunnel tests were fed into the equations of motion [Eqns(1)-(9)] to compute the simulated trajectory. The fourth-order

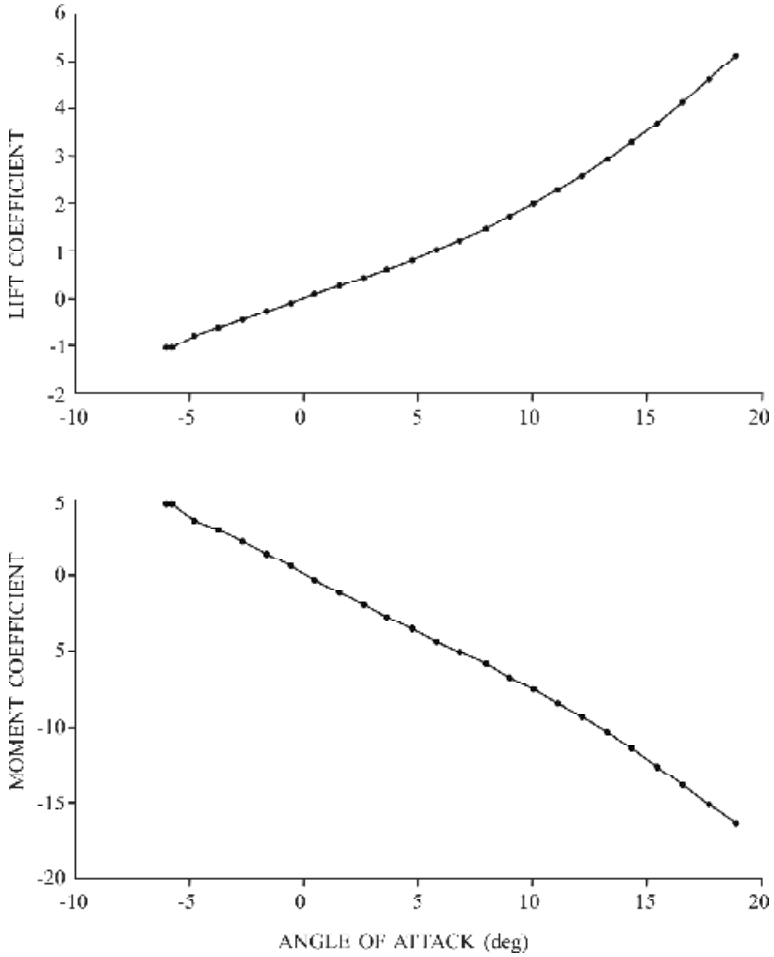

Figure 2. Variations of lift coefficient and moment coefficient with angle of attack for a typical Mach number 0.79.

Runga-Kutta method is employed to integrate Eqns (1)-(9) to generate time histories of position and motion variables.

3. PULSEJET LOGIC AND TUNING PARAMETERS

Lateral pulsejets are used by the flight control system to track a pre-specified command trajectory. For unguided artillery rocket, the command trajectory is downloaded to the rocket just before the launch. The trajectory-tracking flight control system computes the position error by comparing the measured position of the rocket with the commanded trajectory. The computed position error is in the inertial frame of reference. The position error is then converted to the rocket body frame using the following transformation[2]:

$$\begin{bmatrix} e_x \\ e_y \\ e_z \end{bmatrix} = \begin{pmatrix} \cos\theta\cos\psi & \cos\theta\sin\psi & -\sin\theta \\ \sin\phi\sin\theta\cos\psi - \cos\phi\sin\psi & \sin\phi\sin\theta\sin\psi + \cos\phi\cos\psi & \sin\phi\cos\theta \\ \cos\phi\sin\theta\cos\psi + \sin\phi\sin\psi & \cos\phi\sin\theta\sin\psi - \sin\phi\cos\psi & \cos\phi\cos\theta \end{pmatrix} \begin{Bmatrix} x_c - x \\ y_c - y \\ z_c - z \end{Bmatrix} \tag{10}$$

The magnitude and phase of error in the off-axis plane of the rocket are Γ and γ, and are defined by[2]

$$\Gamma = \sqrt{e_y^2 + e_z^2} \tag{11}$$

$$\gamma = \tan^{-1}\left(e_z / e_y\right) \tag{12}$$

The flight control system performs a sequence of checks that govern firing of an individual lateral pulsejet. The conditions that must be satisfied for an individual lateral pulsejet are as follows[2]:

- Magnitude of the off-axis trajectory-tracking error must be greater than a specified distance (e_r):

  $\Gamma > e_r$

- Time elapsed since the last lateral pulsejet firing must be greater than a specified duration (Δt):

  $t - t^* > \Delta t$

- Projected angle between the trajectory-tracking error and the individual pulsejet force under consideration is less than a specified angle (δ):

  $\left|\theta_j - \Pi - \gamma - \phi\left(\Delta_{pj}/2\right)\right| < \delta$

- The individual pulsejet under consideration has not been fired.

  The first two checks are global checks as these are valid for all-lateral pulsejets, whereas the last two checks are specific to a given pulsejet. Primarily for specific applications, the flight control system parameters that need to be tuned are (i) tracking error window size, (ii) required elapsed time between the pulsejet firings, and (iii) angle of tolerance between the tracking error and the individual pulsejet force[2].

4. RESULTS AND DISCUSSION

The rocket configuration used in the study is a routinely used long artillery rocket (2.8 m) having wrap-around fin for imparting flight stability. The lateral pulsejet ring is assumed to be located

0.382 m from the nose tip of the rocket. The main rocket with solid propellant mass (20 kg) burns for around 1.8 s and imparts an average thrust of 22130 N. During the period of acceleration, the forward velocity of the rocket is increased from 40 m/s to 700 m/s. The rocket weight, centre of gravity location from the nose tip, roll inertia, and pitch inertia before and after burnout is 66/46 kg-m^2, 1.40/1.29 m, 0.16/0.13 kg-m^2 and 43/34 kg-m^2, respectively.

For the present study, it is assumed that, nominally, the rocket exists the launcher with the following initial conditions: x = 0 m, y = 0 m, z = 0 m, ϕ = 0°, θ = 5, Ψ = 0, u = 40 m/s, v = 0 m/s, w = 0 m/s, p = 26.17 rad/s, q = 0 rad/s and r = 0 rad/s. Nominal trajectory corresponding to these initial conditions achieves a range (x) of around 4225 m. The nominal command trajectory is the trajectory the rocket seeks to track. This trajectory will be available with the rocket control

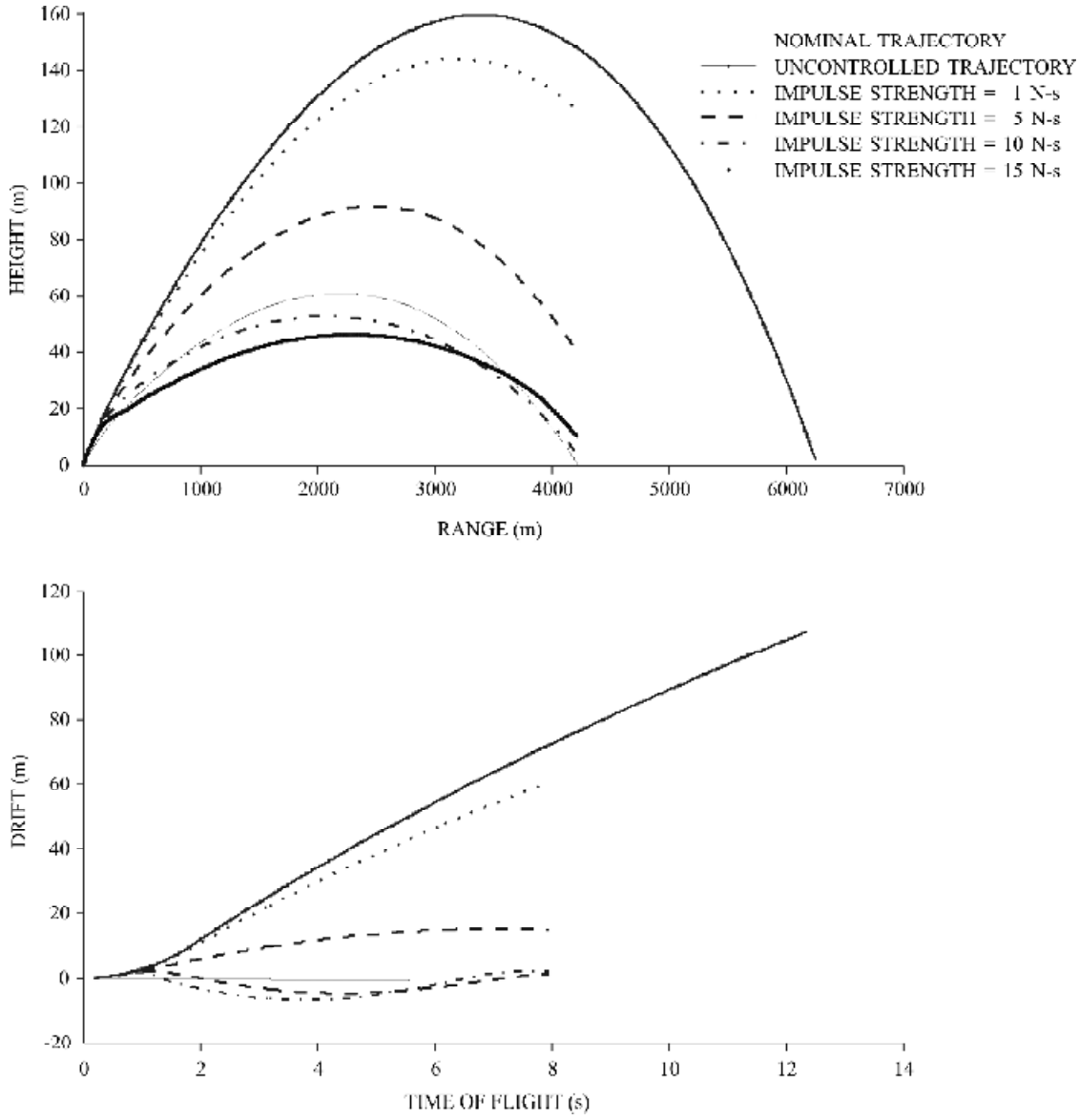

Figure 3. Variations in controlled trajectory parameters for different values of impulsejet strength.

system as reference values of the coordinates (x, y, z) of the centre of gravity of the rocket in motion. The uncontrolled trajectory is the trajectory of the centre of gravity of the rocket in motion, when no pulsejets are fired and the initial error in launching angles are introduced to the model error associated with the launching of the rocket. To simulate uncontrolled trajectory, errors of magnitude 2 and 1° in elevation (θ) and yaw (ψ), respectively are introduced in the initial condition required to generate trajectory by solving equations of motion as given in Eqns(1-9). Controlled trajectory is the rocket's trajectory when pulsejets are fired to align it to the nominal command trajectory. In designing a lateral pulsejet control system, the tuning parameters, namely the number of pulsejets, pulsejet strength (T_j), nominal value of tracking-error window size (e_r), the required elapsed time between the pulsejet firing (Δt), and the angle of tolerance (δ) must be carefully tuned against the desired impact point dispersion level of uncertainty with in the rocket[2]. Various combination of numerical values of tuning parameters were tried to search for an adequate combination of these parameters to reduce the impact point dispersion. Few selective cases are presented in this paper. To start with pulsejet strength

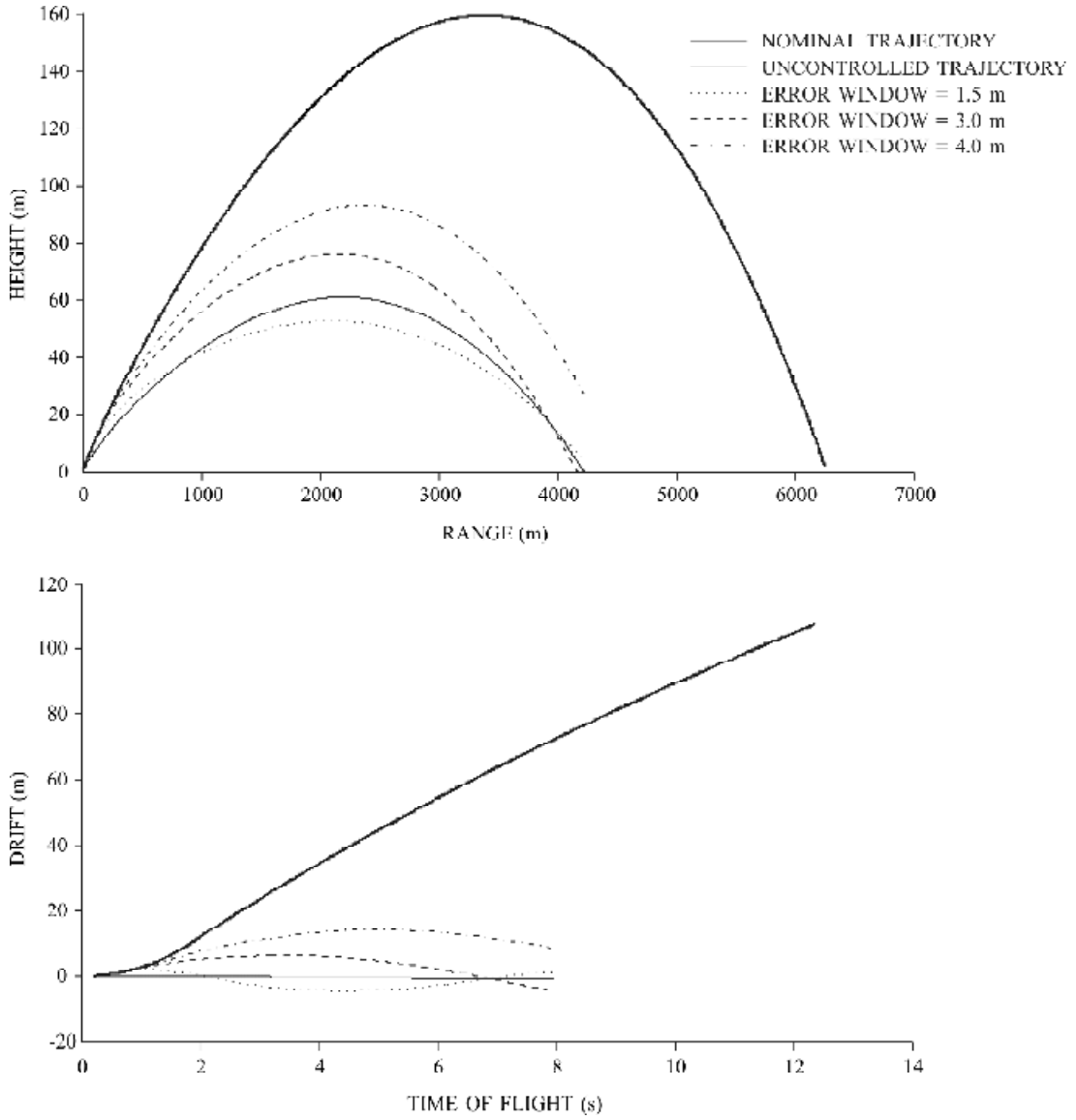

Figure 4. Variations in controlled trajectory parameters for different values of error window size.

of 1,5,10 and 15 N-s were considered. During this exercise, the nominal values for $e_r, \Delta t, \delta$ are kept at 1.50 m, 0.25 s, 1.00°, respectively. It is further assumed that the pulsejet will be operational all throughout the trajectory. The rocket is assumed to be launched at sea level towards a target on the ground with altitude and drift (cross range) equal to zero at a range 4225 m. Figures 3-10 compare uncontrolled and controlled trajectories for the example rocket configuration against a nominal trajectory. The pulsejet ring contains 32 individuals lateral pulsejets, where individual pulsejet strength is varied from 1-15 N-s. Figure 3 plots rocket altitude and drift against range for various values of pulsejet strength. At the target range of 4225 m, the uncontrolled rocket altitude error is around 100 m, and the error in drift is more than 50 m. The commanded trajectories for pulsejets of strength 1, 5, 10, and 15 N-s tend to minimise both the altitude and drift error. It is observed that for pulsejet strength $\geq$ 10 N-s, the controlled trajectory follow the commanded trajectory well within error

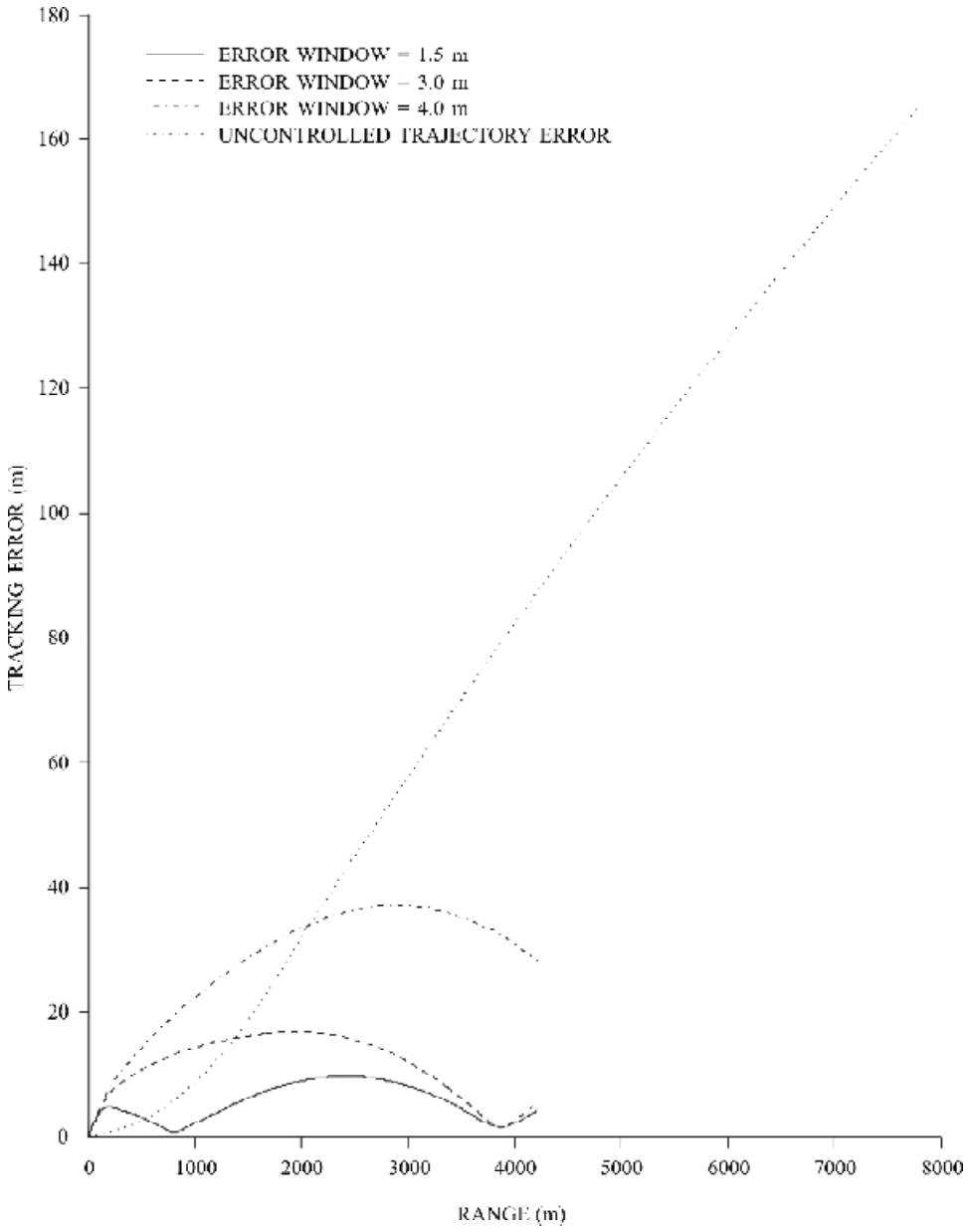

Figure 5. Variations in tracking error for various values of error-tracking window sizes.

of several meters. However, the cumulative error over the whole trajectory is minimum for the case with pulsejet strength of 10 N-s, the altitude and drift errors are 1.05 m and 3.60 m only. Accordingly for this specific application, pulsejet strength of 10 N-s is chosen for further parametric studies. Dispersion reduction is also a strong function of the trajectory window size. To select the error window size, controlled trajectories were estimated separately for error window sizes of 1.5, 3.0 and 4.5 m. During the process of estimation, T_j, Δt and δ were kept fixed at 10 N-s, 0.2 s and 1.0°, respectively.

Figure 4 presents the altitude and drift of the controlled trajectories for various values of error window size. For this-specific application, error window size, e_r of 1.5 m and 3.0 m appear to be adequate. However, for e_r = 4.5 m, the controlled trajectory fails to follow the nominal trajectory at the desired range. Figure 5 presents the variations

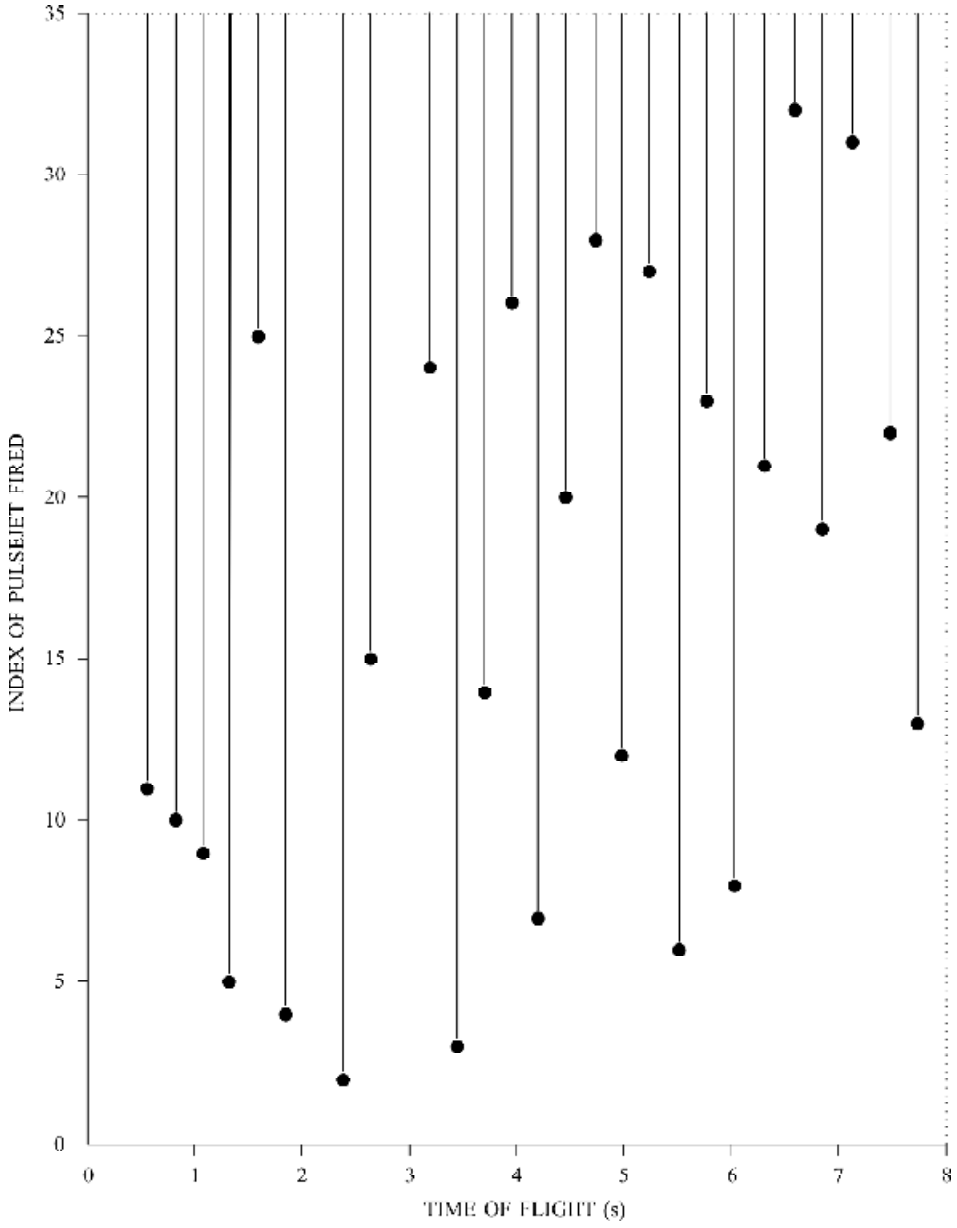

Figure 6. Firing sequence of pulsejet for a controlled trajectory.

of trajectory-tracking error with range. Although, the uncontrolled tracking error exceeded 160 m, the trajectory-tracking error for the lateral pulsejet-controlled rocket with T_j = 10 N-s, e_r = 1.5 m, Δt = 0.25 s and δ = 1.0° remains under 10 m.

The sequence of lateral pulsejet is presented in Fig. 6. Referring to Fig. 6, it can be observed that out of possible 32 lateral pulsejets, 26 were fired in this particular example. It is interesting to note that to follow a 5° nominal trajectory, the command trajectory with chosen tuning parameters would require around 26 pulsejet firings to correct a given specific uncontrolled trajectory. Thus, it is important to have a basic trajectory model perfected/calibrated rigorously with the rocket launcher system before application of pulsejet trajectory-tracking flight control system. The minimum required time between the successive pulses (Δt) is also an important design parameter of the flight control system[2]. If Δt is set too low, the rocket may not have sufficient time to respond, when Δt is set too high only a small number of pulsejets will be fired. In this case, e_r will increase without pulsejet corrective

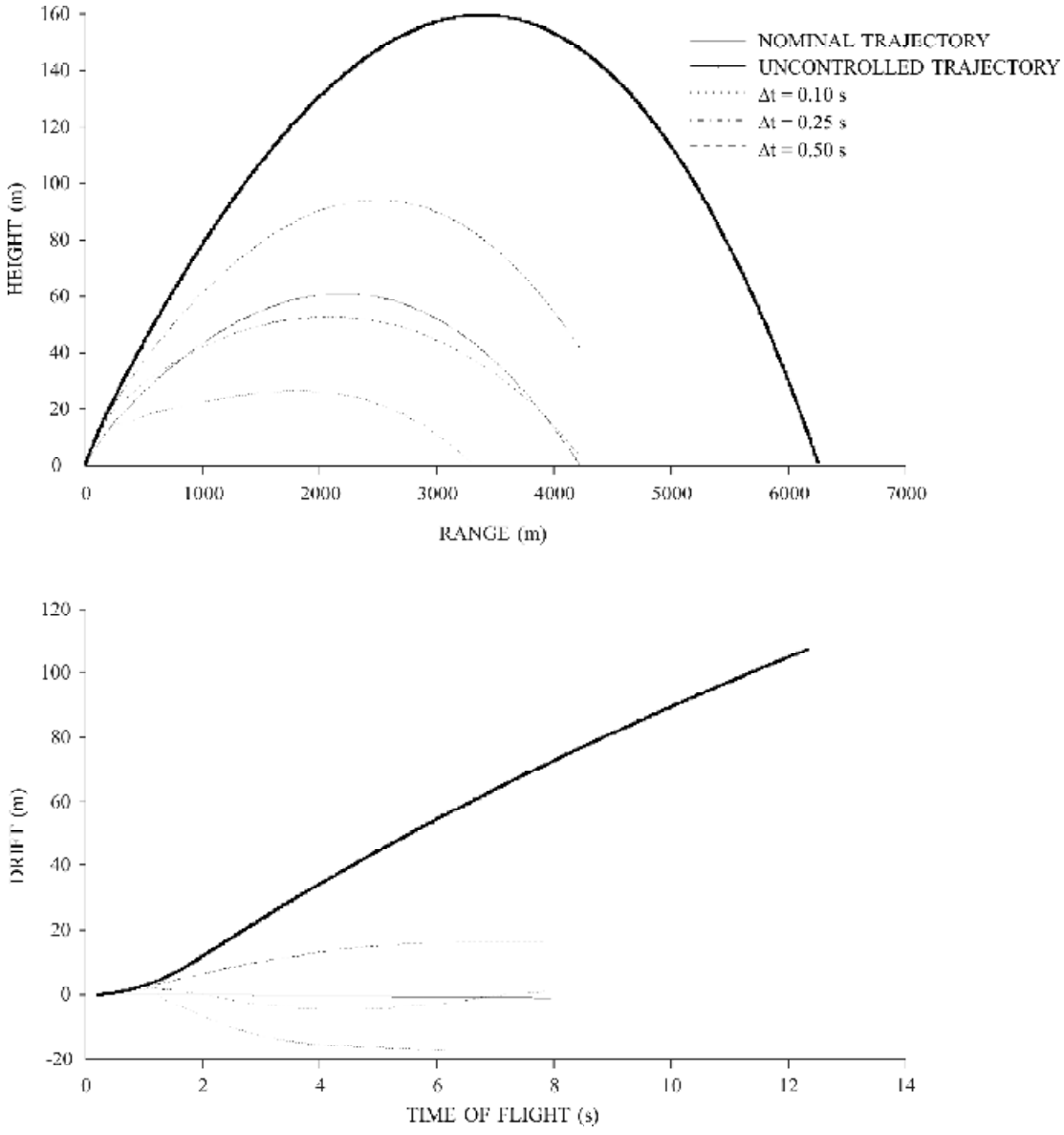

Figure 7. Variations in controlled trajectory parameters for various values of elapsed time.

action. Accordingly, the effect of typical variations in Δt on the performance of controlled trajectory has been studied for this example rocket. A comparison among the controlled trajectories for Δt = 0.10, 0.25 and 0.50 s for a given T_j = 10 N-s, e_r=1.5 m, δ=1.0°, has been presented pictorially in Fig. 7. Referring to Fig. 7, it can be observed that for low value of Δt = 0.1 s and for relatively higher value of Δt = 0.5 s, the controlled trajectory fail to achieve the desired impact point correction. For Δt = 0.25 s, the error in altitude and drift were 3.6 m and 2.0 m, respectively. The altitude and drift error for Δt = 0.1 s and 0.5 s are several meters larger than the corresponding value of these errors for Δt = 0.25 s.

It is important to fine-tune the value of pulsejet angle threshold, δ for efficient use of pulsejet logic. Figure 8 presents a comparison between the nominal and the controlled trajectories for different values of pulsejet angle threshold, δ. The controlled trajectories initiated with δ = 0.1, 1.0 and 10.0° yield acceptable impact point error. Although, δ = 0.1° yields comparatively better results, however,

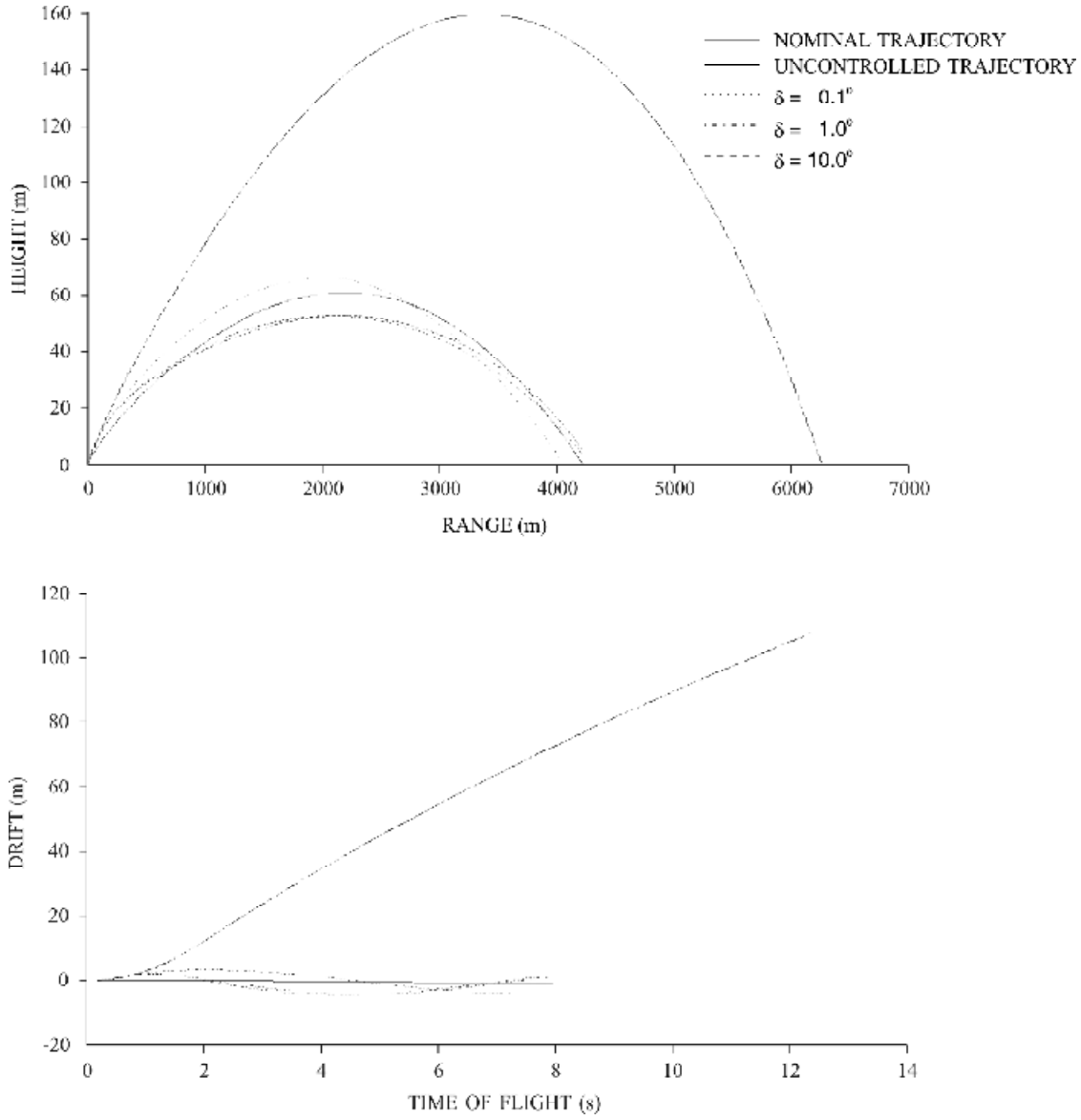

Figure 8. Variations in controlled trajectory parameters for various values of pulsejet angle threshold.

keeping low-cost instrumentation in mind, $\delta = 1^{o}$ was frozen as one of the tuning parameters.

Figure 9 presents a comparison between the pitch attitude of uncontrolled and the controlled trajectories of the example rocket. It is observed that nominal and uncontrolled pitch attitude steadily decreases as the rocket flies down range. However, as expected, the controlled trajectory showed an oscillatory response due to the firing of pulsejets. Similar oscillations were also seen in the yaw angle-range history shown in Fig. 10.

To identify the desired position of flight path required, three separate controlled trajectories were computed assuming that the pulsejet were operative all throughout the flight; the pulsejet were operative only up to boost phase; the pulsejet were operative during terminal phase of the trajectory (after 4.5 s from launch). Figure 11 presents comparison among the controlled trajectories for all the three cases.

Referring to Fig. 11, it can be seen that the controlled trajectory, when pulsejet logic is operative

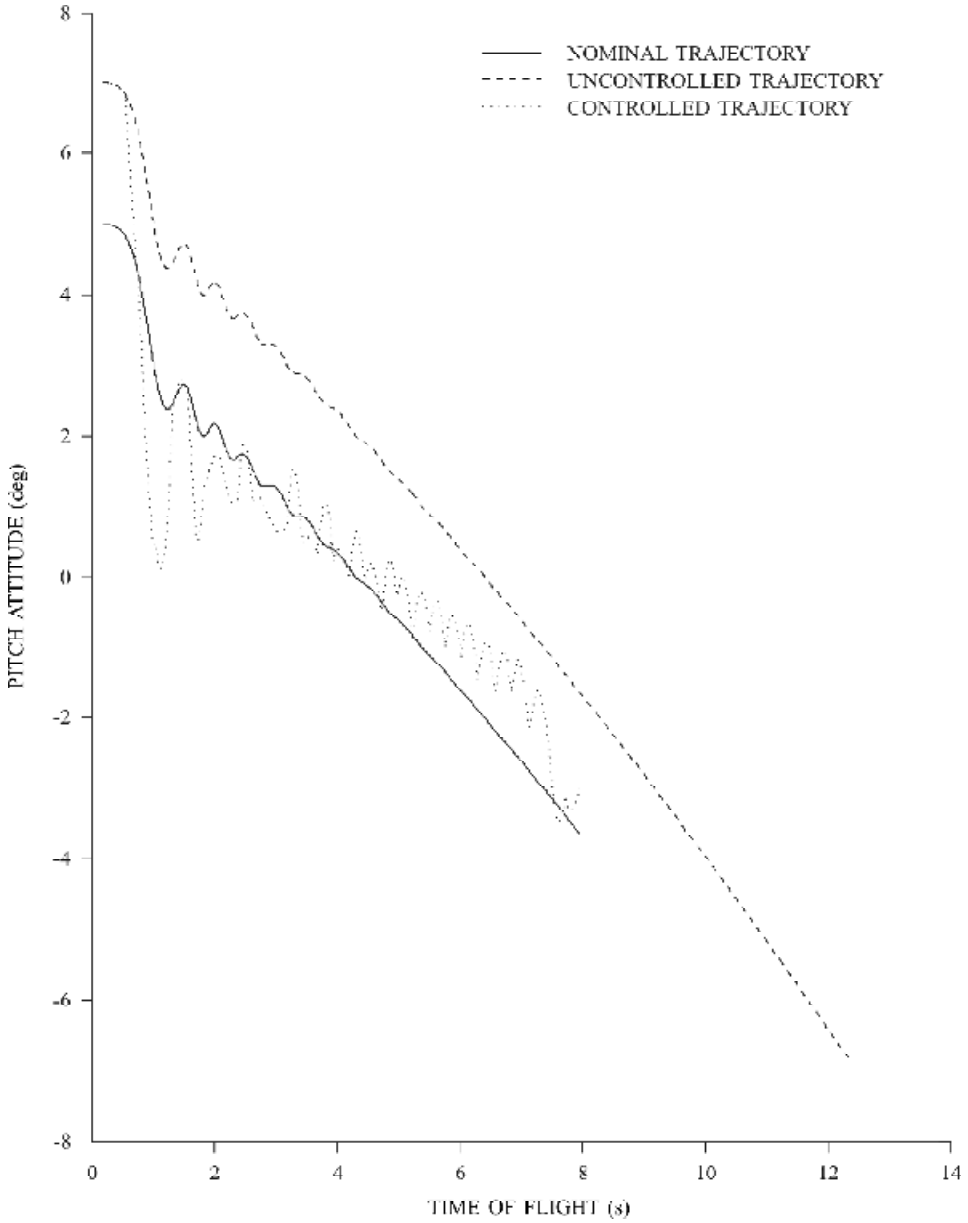

Figure 9. Comparison in pitch attitude for nominal, uncontrolled, and controlled trajectories.

all throughout the trajectory, yields minimum impact error. It is interesting to see that the controlled trajectory corresponding to the case when pulsejet logic is operative up to boost phase (T=1.8 s) also yields fair amount of reduction in impact point dispersion. From practical application point of view, this observation can play a critical role in designing a suitable low-cost control system for the specific application. In artillery rocket firing to engage a given target, the correction required in rocket's elevation and yaw (azimuth), to compensate the effect of wind and metrological variations during boost phase are much larger than the correction required during free-flight phase. Application of pulsejet logic during the boost phase can result in large reduction in cost and complexities of the control system.

To study the effect of measurement noise on the performance of the pulsejet logic for the specific application, simulated pseudo noise of varying intensities are added to the simulated range (x), altitude (z), and drift (y). The noise is simulated by generating successively uncorrected pseudo random numbers having normal distribution with zero mean and assigned

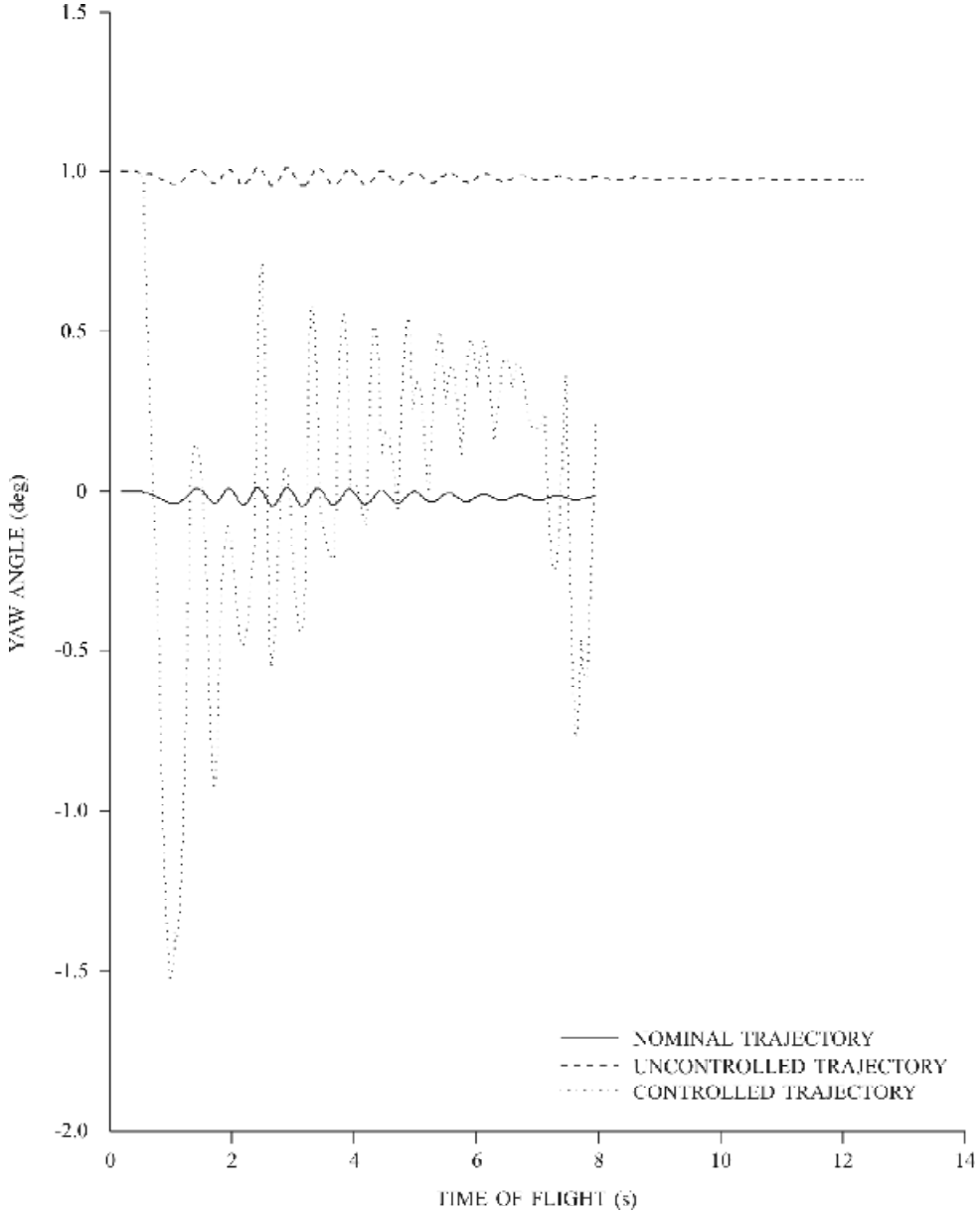

Figure 10. Comparison in yaw angle for nominal, uncontrolled, and controlled trajectories.

standard deviation corresponding to a designated percentage (5 % and 10 %) of the chosen possible maximum error expected based on the type of instrumentation being used. For this specific case maximum error expected in *x*, *y* and *z* has been restricted to 35 m only. Controlled trajectories with 5 per cent and 10 per cent noise are generated and the impact error in altitude and drift are presented in Table 1. Referring to Table 1, it can be observed that the altitude error increased with the increase in noise level in measurement of *x*, *y* and *z*.

Table 1. Variation in error in range, height, and drift due to increase in measurement noise

Measurement Noise %	Error in Range *X* (m)	Height *Y* (m)	Drift *Z* (m)
0%	-2.7	3.63	-2.27
5%	-2.7	0.42	2.10
10%	-2.9	-12.70	-1.27

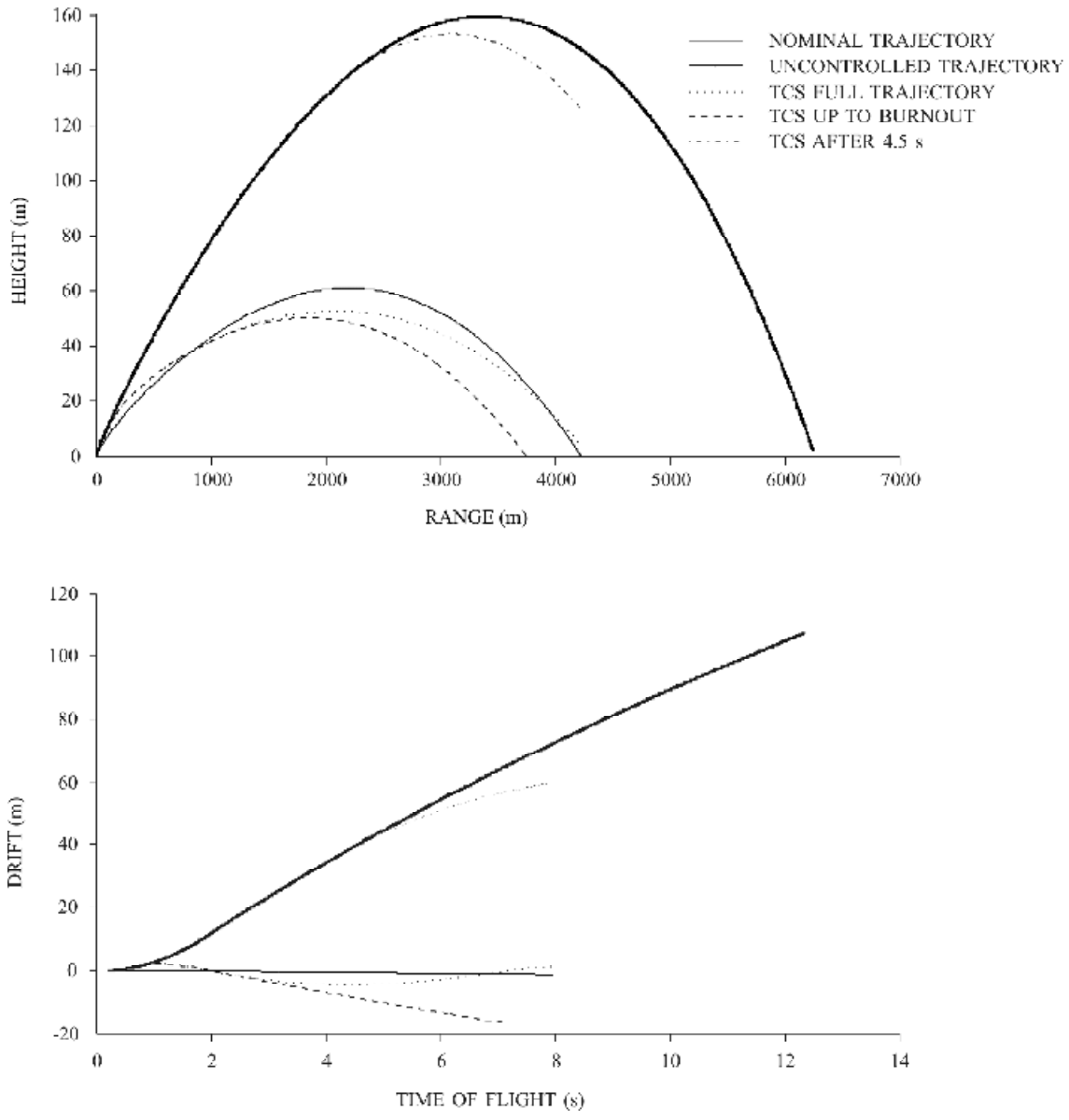

Figure 11. Variations in trajectory parameters due to different time of execution of trajectory correction system.

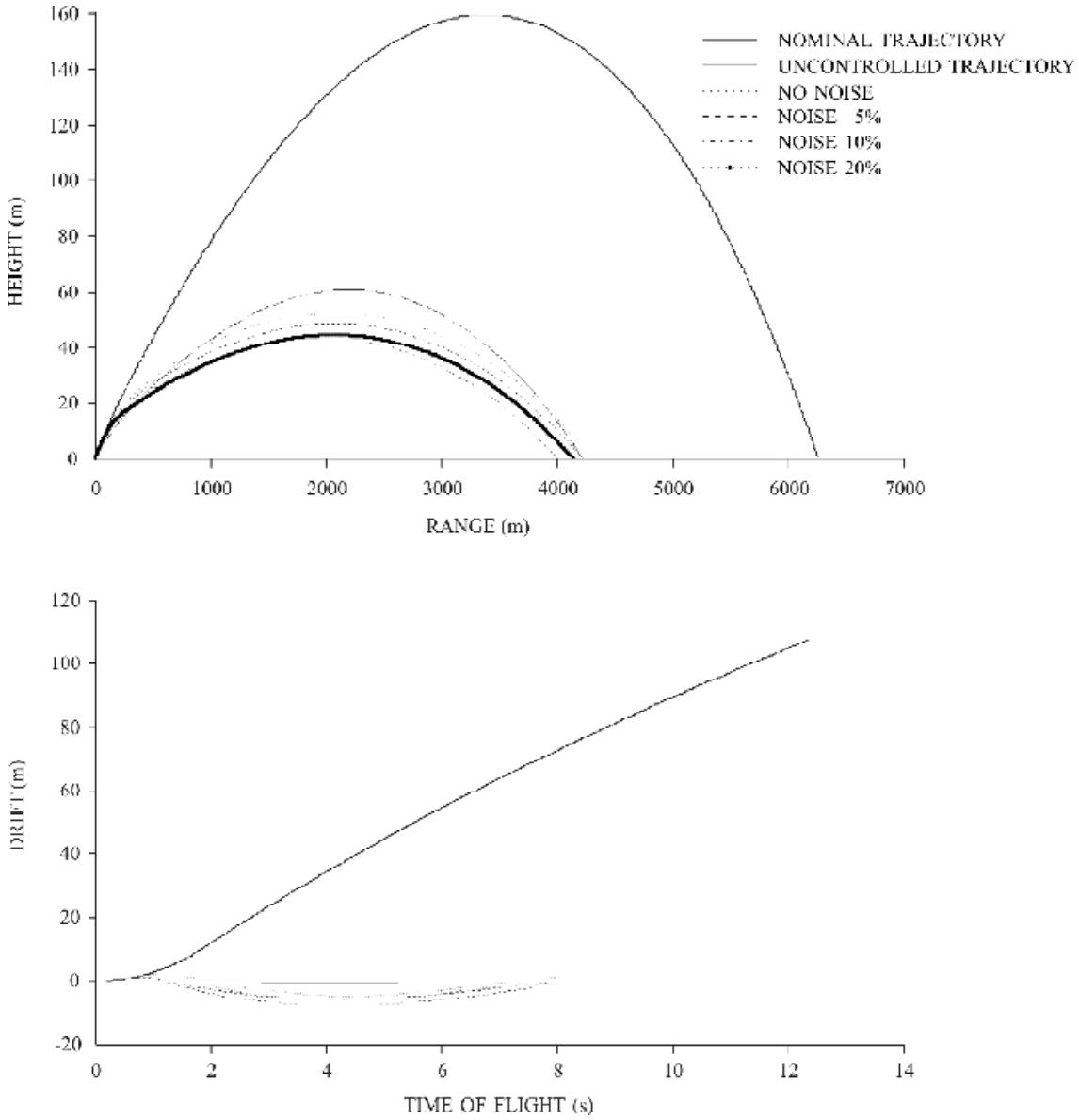

Figure 12. Variations in dispersion of trajectory parameters due to noisy measurement.

A comparison of e_z and e_y of control trajectories for noise level of 5 per cent and 10 per cent are presented in Fig. 12. It can be seen that the presence of 10 per cent noise deteriorated the impact error as compared to control trajectories having noise of around 5 percent in the measurement.

5. CONCLUSIONS

The study has been undertaken to explore the feasibility of reducing the impact point dispersion of a routinely used artillery rocket using lateral pulsejets coupled to a trajectory-tracking flight control system. Simulation studies were conducted to arrive at tuning parameters, namely the tracking-error window size, the required elapsed time between the pulsejet firings, and the angle of tolerance between the tracking error and the individual pulsejet force. The numerical values of the tuning parameters required for the chosen example artillery rocket were estimated by applying pulsejet logic to reduce the impact point dispersion. Further, the robustness of the methodology wrt measurement noise has also been evaluated for the example artillery rocket.

ACKNOWLEDGEMENTS

The authors acknowledge the support provided by the Armament Research Board, R&D DRDO, HQrs, New Delhi, for the above study.

REFERENCES

1. Anonymous. External ballistics. *In* Text book of ballistics and gunnery, Vol. 2. Her Majesty Stationary Office (HMSO), London, 1987. pp. 443-97.

2. Jitpraphai, Thanat. & Costello, Mark. Dispersion reduction of a direct fire rocket using lateral pulse jets. *J. Spacecraft Rocket*, 2001, **38** (6), 929-36.

3. James, L. Robert (Jr) & Harris, J. Ronald. Calculation of wind compensation for launching of unguided rockets. NASA, Washington, D.C., Report No. NASA-TND-645.

4. Dehury, Santosh Kumar. Modelling of performance of an artillery shell using neural networks. IIT, Kanpur, 2000. MTech Thesis.

5. Om Prakash. Modelling of performance of an artillery rocket using feed-forward neural networks. IIT, Kanpur, 2002. MTech Thesis.

6. Waszak, M. R. & Schmidt, D. K. Flight dynamics of aeroelastic vehicles. *Journal of Aircraft*, 1988, **25** (6).

7. Richard, E. Maine. & Kenneth, W. Iliff. User's manual for MMLE3, a general FORTRAN program for maximum likelihood parameter estimation. Dryden Flight Research Centre Edwards, California. NASA Technical Paper No. 1563.

8. Richard, E. Maine. & Kenneth, W. Iliff. Application of parameter estimation to aircraft stability and control.

9. Harkins, T.E. & Brown, T.G. Using active damping as a precision enhancing technology for 2.75 in. rockets. Aberdeen Proving Ground, MD, 1999. US Army Research Lab., ARL Report No. TR-1772.

10. Anthony, J. Calise & Hesham, A. El-Shirbiny. An analysis of aerodynamic control for direct fire spinning projectiles. *In* AIAA Guidance, Navigation and Control Conference, 2001.

11. Platus, D.H. Aeroelastic stability of slender, spinning missiles. *J. Guid. Cont. Dyn.*, 1992, **15** (1), 144-51.

12. Meirovitch, L. & Nelson, H.D. On the high-spin motion of a satellite containing elastic parts. *J. Spacecraft Rocket*, 1966, **3**, 1597-1602.

13. Oberholtzer, N.W.; Schmidt, L.E. & Larmour, R.A. Aeroelastic behaviour of hypersonic reentry vehicles. AIAA Paper No. 83-033, 1983.

14. Kirsch, A.A. Dynamic equations of motion for flexible vehicles. General Electric Co, Philadelphia. US Patent No. TIS-65SD310. 12 August 1965.

15. Bennighof, J.K. & Subramanium, M. Minimum time manoeuvre of flexible systems using pulse response-based control. *J. Guid. Cont. Dyn.*, **20** (1), 1997, 129-36.

Contributors

Mr Ankur Singhal is working as Research Associate in the Department of Aerospace Engineering at the Indian Institute of Technology (IIT), Kanpur. He is working in the area of flight mechanics.

Dr A.K. Ghosh did his MTech and PhD both from IIT, Kanpur. Presently, he is the Faculty Incharge, Flight Laboratory at the Institute. His areas of interest are: Flight mechanics, flight testing, parameter estimation from real flight data, and neural networks.